10.1109/ULTSYM.2012.0099

Numerical and experimental classification of the oscillations of single isolated microbubbles: occurrence of higher order subharmonics

Amin Jafari Sojahrood, Raffi Karshafian, Michael C. Kolios

[#]*Department of Physics, Ryerson University, Toronto, Ontario, Canada*

Abstract— **Imaging and therapeutic applications of microbubbles (MBs) in medical ultrasound are rapidly increasing. Despite the many theoretical and experimental investigations of MB dynamics, theMB behavior is considered to be very complex and difficult to control. The optimization of microbubble composition and ultrasound exposure parameters requires detailed knowledge of the behavior of MBs over a large range of the control parameters of the system (e.g. pressure, frequency, MB size, MB shell composition). In this work, the dynamics of microbubbles consisting of viscoelastic shells were studied both numerically and experimentally. Polydisperse dilute solutions of Artenga MBs (Artenga Inc.) were sonicated at the frequency of 25 MHz using pulse trains of 30 cycles with a Vevo770 ultrasonic machine. For each sonication the driving pressure were varied between 100 kPa to 3.8 MPa. The backscatter signals from single MBs were isolated and analyzed further. The Hoff model for viscoelastic shell MBs was numerically solved for a wide range of MB sizes and driving acoustic pressures at 25 and 55 MHz. The results of the numerical simulations were visualized using bifurcations diagrams (MB expansion ratio versus MB size and acoustic pressure). The bifurcation structure of the viscoelastic MBs, to our best knowledge for the first time, classified the dynamics over a large range of exposure parameters, predicting the existence of higher order subharmonics. In agreement with experimental observations, simulations predict the generation of oscillations including period 2, period 3, period 4 and period 5 in the case of the sonication of polydisperse MB sizes at pressure values above specific thresholds. Another interesting finding is the differentiation between different regimes of period 4 oscillations, observed both experimentally and numerically. Numerical simulations reveal that depending on the MB size, an increase in acoustic pressure can result in oscillations that can undergo two successive period doublings from period two to period 4 or directly from period one to period 4. The dynamic characteristics of these two types of oscillations are for the first time studied in detail. In addition, frequency analysis of the ring-down oscillations of the MBs in experiments is in good agreement with the size predictions of the numerical simulations. The higher period oscillations from bigger MBs at higher frequencies may provide significant advantages for imaging, drug delivery and clot lysis ultrasound applications. These include stronger SHs or UHs signals which are closer to the transducer resonant frequency and higher and longer lasting shear stresses on the nearby cells.**

***Keyword*-Viscoelastic Microbubbles, Subharmonic Imaging, Drug delivery**

I. INTRODUCTION

Contrast enhanced ultrasound (CEUS) provides a real time, non-invasive and cost-effective modality for imaging the blood flow in the tissue. Through isolating the nonlinear frequencies of ultrasound contrast agents (UCAs), the signal of the tissue can be suppressed and the contrast to tissue ratio (CTR) can be increased. Detecting the subharmonic (SH) frequency in the backscatter signal provides the highest CTR, compared to all the other nonlinear imaging modalities [1]. This is because tissue backscatter cannot produce SH frequencies [1]. However, SH imaging may suffer from low resolution and sensitivity. The former limitation is because the frequencies of sonication are determined by twice the resonance frequency (fr) of the UCA and therefore the detection is typically performed at half the transmit frequency. The limited transducer bandwidth results in reduced detection sensitivity for the subharmonic signal produced. Increasing the transmit frequency or increasing the sensitivity of the detection of SH signals can improve the performance of the SH imaging. In order to design novel SH imaging procedures with higher resolution and sensitivity, a more comprehensive understanding of the dynamics of the UCAs at higher frequencies is required. To accomplish this, we have numerically classified the dynamics of UCAs for a wide range of system parameters (UCA properties and transmit frequency and pressure). To confirm these predictions, experiments are performed using Artenga UCAs.

II. METHODS

A. Numerical simulations

The dynamics of the UCAs were simulated using the Hoff model [2]:

$$\rho_L(\ddot{R}R+\frac{3}{2}\dot{R}^2)=P_0\left((\frac{R_0}{R})^{3\Gamma}-1\right)-p_A(t)-4\mu_L\frac{\dot{R}}{R}-12\mu_s\Theta\frac{{R_0}^2}{R^3}\frac{\dot{R}}{R}-12G_s\Theta\frac{{R_0}^2}{R^3}(1-\frac{R_0}{R}) \quad (1)$$

where R_0 is the initial radius, ρ_L is the density of the liquid, P_0 is the equilibrium pressure inside the bubble, Γ is the polytropic exponent, μ_L is the viscosity of the surrounding liquid, μ_s is the shell viscosity, Θ is the shell thickness and G_s

is the shear modulus. $p_A(t)$ is the driving acoustic pressure and is given by equation 2:

$$p_A(t) = P_A \sin(2\pi f t) \quad (2)$$

The results of the numerical simulations were visualized using a bifurcation analysis, a method used commonly in non-linear physics [3]. In this method the bifurcation structure of the normalized UCA oscillations (R/R0) are plotted versus a control parameter [3]. This gives insight into the nonlinear MB behaviour over a wide range of parameter, thus reducing the complexity of the analysis and interpretation of the results.

B. Experiments

The experimental verification of the results was done through sonicating a polydisperse dilute solution of Artenga UCAs, with continuous pulse trains of 30 cycles at25 MHz frequency for pressures values of ~0.1-2.5 MPa, generated by a Vevo 770 ultrasound instrument (VisualSonics Inc. Toronto, Ontario). The dilute solution enabled the recording of single scattering events from individual MBs. The backscattered signal from each single UCA within the focus of the ultrasound transducer was recorded and different nonlinear modes of oscillations were identified.

III. RESULTS

A. *Numerical simulations*

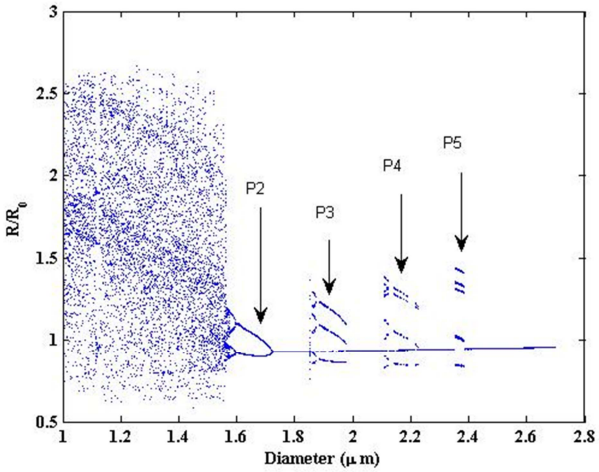

Fig. 1 Bifurcation structure of the normalized MB oscillations (R/R0) with respect to MB initial diameter. The sonication frequency is 25MHz, acoustic pressure is 2.54MPa.

To better understand the nature of the complex signals that we expect by sonicating a polydisperse population of UCA sizes, here, we have presented the bifurcation diagram of a sample UCA (Gs= 50 MPa, μ_s=0.062 nm, and Θ = 3nm) versus the MB size at different pressures while keeping the frequency of the sonication fixed at 25 MHz. We observed that for a sufficient driving pressure, different nonlinear modes of the MB oscillations can manifest themselves in the bifurcation diagram. Figure 1 shows a representative case of the bifurcation structure for an ultrasound exposure (2.54MPa peak pressure). For smaller MBs the chaotic oscillations dominate the MB behaviour and the oscillation amplitude surpasses a predicted destruction threshold (R/R0>2 [4]). For larger MB sizes (~1.56-1.86 μm) the oscillations undergo successive reverse period doublings from chaotic oscillations to period 4 (P4-2), then P2 and finally P1 oscillations. We designate the P4 oscillations of the small MBs type 2, and this will be discussed shortly after. As illustrated in fig. 1, the broad range of MB sizes exhibiting P2 oscillations is followed by 4 distinct MB size ranges for the MB sizes examined. These regions include MB sizes exhibiting linear, P3 (~1.90-1.97 μm), P4-1(~2.14-2.23 μm) and P5 (~2.35-2.39 μm) oscillations. The P3, P4 and P5 oscillations result in the generation of higher order SHs in the backscattered signal [3]. To our best knowledge this is the first published study of the classification of the dynamics of the MBs that demonstrate these higher order SHs. The resonance sizes of the MBs capable of exhibiting P_m oscillations is approximately slightly more than or equal to the size of the MB that corresponds to a natural resonance at $\frac{1}{m}$ (m=2,3,..) of the driving frequency.

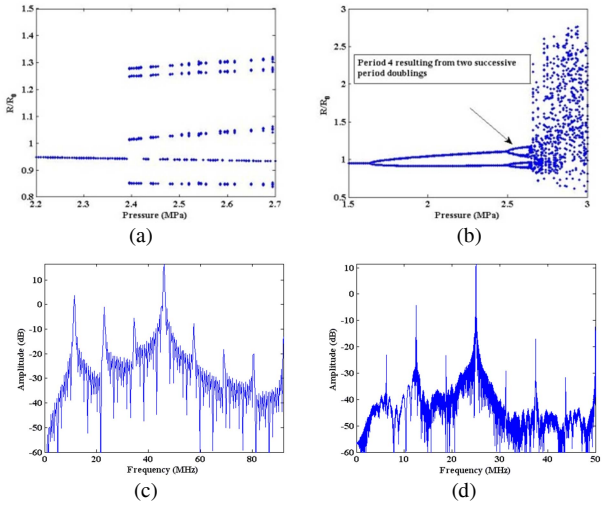

Fig. 2 Bifurcation structure of the normalized UCA radius versus pressure for a) 2.16 and b) 1.6 micron UCAs. The corresponding frequency spectrum of the backscatter signal at 2.54 MPa of: c)2.16 and d)1.6 micron UCAs.

It also should be emphasized that, there is a fundamental difference between the two period 4 oscillations of type 4-1 and 4-2. This difference is studied in more detail in figure 2. The resonance frequency of the MBs exhibiting P4-1 oscillations is approximately 1/4 or slightly more than 1/4 of the ultrasound driving frequency. As a representative case one can consider a 2.16 μm diameter MB. The natural resonance frequency of this MB is 6.58 MHz and according to fig. 1 is capable of exhibiting P4-1 oscillations. In fig. 1, the smaller MBs exhibiting P4-2 oscillations have a resonant frequency larger than 1/2 of the driving acoustic frequency. As a representative case consider a 1.59 μm MB which according to figure 1 exhibits P4-2 oscillations. This MB has a resonance frequency of 20.02 MHz. Fixing the frequency at 25 MHz; the bifurcation structure(R/R0 versus pressure) of the 2.16 μm and

1.59µm MB are plotted in figure 2a and 2b, respectively. As seen in fig 2a, as the pressure increases above a certain threshold, the oscillations undergo a direct transition from P1 to P4 oscillations. However in fig 2b, by increasing the pressure above a threshold, the P2 oscillations undergo period doubling bifurcations to P4 oscillations. Therefore, the main difference between P4-1 and P4-2 oscillations is that P4-1 is the result of direct transformation from period 1 to period 4 while P4-2 is the result of two successive period doubling oscillations from period 1 to period 4. To gain a better insight on the difference between the two types of P4 oscillations, the frequency spectra of the backscattered pressure of the two MBs at 2.54 MPa are plotted in figure 2c and 2d.The frequency response of both the P4-1 (fig. 2c) and P4-2 oscillations (fig. 2d) contains 3 SHs. The order of the scattering strength of the SHs in the oscillations of a MB undergoing P4-1 oscillations, is ¼ (6.25MHz) > 2/4 (12.5MHz) > ¾ (18.25 MHz). This is different from the SH strength order of the P4-2 oscillations. The order of the strength of the SHs in the case of the P4-2 oscillations is 2/4 (12.5MHz) > 3/4 (18.25 MHz)> ¼ (6.25MHz).

A. Experimental observations

In order to highlight experimental observations of the nonlinear signals shown in figure 1 and figure 2, representative measured RF signals are presented in figure 3 and figure 4. Figure 3a shows a representative case of a period 2 signal, a MB oscillation which undergoes period doubling and represents the dynamics of the UCAs in conventional SH imaging. The RF signal has 2 distinct maxima, in good agreement with numerical predictions. The corresponding frequency spectrum in figure 3b shows a strong SH content at 12.5 MHz. A representative case for P3 oscillations is illustrated in figure 3c. The signal has three distinct maxima and the frequency spectrum of the signal in figure 3d has 2 distinct SHs of orders of 1/3(8.33MHz) and 2/3 (16.66 MHz).The backscatter from P5 oscillations is presented in figure 3e. The signal has 5 distinct maxima and the frequency spectrum of the signal has SHs of the orders of 1/5 (5MHz), 2/5(10 MHz), 3/5 (15 MHz) and 4/5 (20 MHz). Both of the detected P4 oscillations are highlighted separately in figure 4. Fig.4a illustrates the oscillations of P4-2 type. The RF signal has four distinct maxima and the corresponding frequency spectrum has 3 distinct SHs of the orders of 1/4 (6.25MHz), 2/4 (12.5MHz) and 3/4 (18.75 MHz). Figure 4b shows an example of the P4-1 oscillations. Again in agreement with numerical simulations the signal has 4 distinct maxima and the corresponding frequency spectrum (figure 4d) has 3 distinct SHs of the orders of 1/4 (6.25MHz), 2/4 (12.5MHz) and 3/4 (18.75 MHz).

One of the most interesting results of this work is that we were able to experimentally verify the numerical characterization (fig 2) of the two period 4 types for the first time. In line with the numerical results, there were two types of the period 4 signals with a different pattern of the repetition

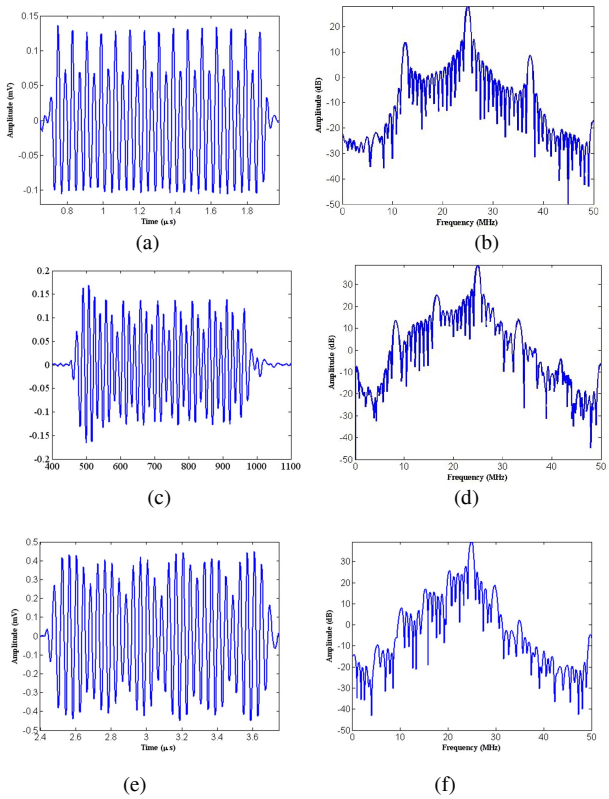

Fig. 3: Experimental detected backscatter signal from isolated Artenga UCAs right column, and their corresponding frequency spectrum left column.

of the maxima and minima (figure 4a and 4b). Figure 4a shows the experimentally detected period 4 signals which are likely related to the oscillatory pattern labeled as P4-1 in figure 2a. The backscatter maxima in the frequency spectrum of the P4-1 oscillation pattern has 3 SHs with the strength order of 3/4>2/4>1/4. The frequency spectrum of the P4-2 oscillations (figure 2d and 4d) has SHs with the strength order of 2/4>3/4>1/4. This reveals the similarity between experiments and the numerical simulations. In the experiments, the SH of order 2/4 is stronger than the SH of 3/4 and the order ¼ cannot be effectively detected.

The numerical simulations (figure 2a-d) and the transducer response can be used to explain why there is an absence of a strong SH of the 1/4 order in the experimental results presented in figure 4d. Numerical simulations predict the strength order of the SHs in P4-1 oscillations as 1/4>2/4>3/4. However in experiments the transducer is not able to detect all the SHs with the equal sensitivity. The sensitivity of the transducer in detecting the signals decreases as for frequencies lower than the central frequency of the transducer (25 MHz). If the transducer sensitivity as a function of frequency is taken into account, the actual detected strength of the SHs for P4-1 oscillations is 1/4>2/4>3/4.

In case of the P4-2 oscillations, numerical simulations predict the strength of the SHs as 2/4>>3/4>1/4. The 1/4 SHs are very weak (-40dB below the fundamental). Therefore the transducer is likely not able to detect this frequency properly as the sensitivity of the 25 MHz VEVO transducer at 6.25 MHz is weak. Therefore, there is an absence of a strong peak

at 6.25 MHz in figure 3f. However, the 1/2 SH is still stronger than the 3/4 SH, even though the transducer is more sensitive at the 3/4 SHfrequency. This is due to the high strength of the 1/2 order SH predicted inthe numerical simulations. Even though the transducer sensitivity is higher at the frequency of the 3/4 SH, the 1/2 order SH was still stronger than the 3/4 SH.

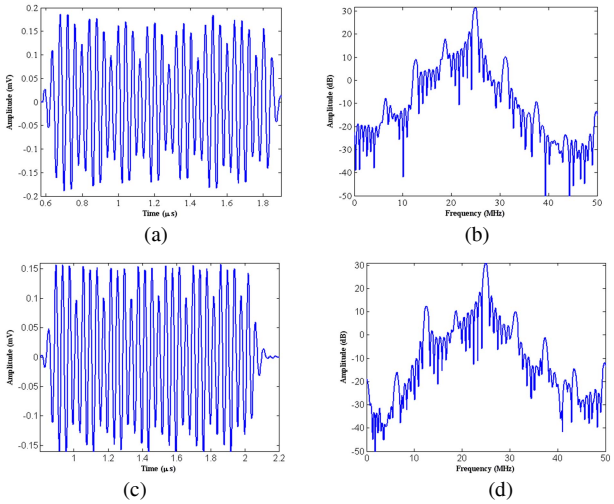

Fig. 4 Two type of the experimentally detected period 4 oscillations right column and the corresponding frequency spectrum left column

A critical parameter in predicting the response of the MB is the initial MB size, yet in the experiments the MB size is not known; for a particular RF signal the MB size that generated this signal is not known. However, the free natural oscillations of the MB at the end of the acoustic exposure can provide information about the natural resonance frequency of bubble – this is also known as the MB ring-down. In the ring-down analysis, only signals with an SNR above 12.7dB were considered (to ensure adequate SNR). The ring down analysis of the 11 P2 signals recorded that met this criterion and the 10 P3 signals resulted in calculated resonance frequencies of 14.53±3.02 MHz and 9.53±1.37 MHz, respectively. These results are consistent with the numerical predictions for MBs of this size and these types of oscillations detected (Figure 2). It should be noted that because of the decreased sensitivity of the transducer, we were not able to obtain clear ring down signals for P4 and P5 signals with adequate SNR. The analysis of the two ring-down signals with the greatest SNR for the P4 and P5 oscillatory patterns resulted in calculated resonance frequencies of 7.38 and 4.98 MHz respectively. This again is consistent with the theoretical predictions of Figure 2.

IV. Discussion

The dynamics of the MBs undergoing nonlinear oscillations were numerically and experimentally classified. Numerical bifurcation diagrams of the radial oscillations of the MB versus its initial size reveals that at sufficiently high enough pressures, MBs can undergo different modes of nonlinear oscillations and exhibit higher order SHs. In this regard, the resonance sizes of the MBs capable of exhibiting SHs oscillations of order *m* is approximately slightly more than or equal to the size of the MB that corresponds to a natural resonance at $\frac{1}{m}$ (m=2,3,..) of the driving frequency. Experimental observations of the backscattered signal from single MBs verified the numerical predictions.

The findings of this study may ultimately provide information for improving agent detection and refining the current methods in contrast enhanced applications. Higher order SHs can be generated at higher frequencies compared to conventional SHs. In addition they are closer to the fundamental frequency transmitted by the imaging transducer which may increase the detection sensitivity. Another interesting property of these oscillations is their stability (R/R0<2 [4]). As the shear stress around the oscillating MBs is proportional to the driving frequency$^{3/2}$, MBs oscillating in the regime of higher order SHs may be responsible for higher shear stresses on the nearby cells. Considering the strong stable non collapsing oscillations, this regime may provide long lasting high shear stresses on the nearby cells, thus it may enhance the sonoporation efficacy in MB drug delivery applications and further studies can be designed to investigate this phenomenon.

V. Conclusion

Nonlinear dynamics of the UCAs with viscoelastic shell undergoing higher order SHs were classified using numerical simulations and the results were experimentally verified.

VI. Acknowledgement

Funding for this work has been provided by the Canadian Institutes of Health Research (CIHR) grant MOP-97959, a program project grant from the Terry Fox Foundation/CIHR entitled “Ultrasound for Cancer Therapy” and the Canada Research Chairs Program.

References

[1] P.M. Shankar, P.D. Krishna, V.L. Newhouse, Advantages of subharmonic over second harmonic backscatter for contrast-to-tissue echo enhancement Ultrasound Med Biol, 24 (1998), pp. 395–399

[2] 2- Hoff, L., Sontum, P.C., and Hovem, J.M. Oscillations of polymeric microbubbles: Effect of the encapsulating shell. J. Acoust. Soc. Am., 107(4), (2000) 2272-2280.

[3] 3-Amin Jafari Sojahrood, Michael C. Kolios, Classification of the nonlinear dynamics and bifurcation structure of ultrasound contrast agents excited at higher multiples of their resonance frequency, Phys. Lett. A, 356, (2012), 2222-2229

[4] 4- Flynn, H.G., and Church C.C. Transient pulsations of small gas bubbles in water. Journal of the Acoustical Society of America, 84, (1988), 985-998.